BIFURCATION AND FRACTURE IN REINFORCED-CONCRETE SPECIMENS UNDER COMPRESSION

K. Ikeda and Y. Yamakawa
Department of Civil Engineering, Tohoku University, Sendai, Japan
K. Maruyama and M. Emoto
Department of Civil Engineering, Nagaoka University of Technology
Nagaoka, Japan

Abstract The fundamental mechanism of the compressive behavior of cylindrical concrete specimens reinforced by steel fibers is explained through a dual viewpoint of bifurcation and fracture. Asymptotic bifurcation theory is employed as a means to testify if the bifurcation that triggers the softening of the stress versus strain curves of specimens is taking place or not. These curves are classified into two categories: their peak loads are governed by (1) bifurcation and by (2) splitting or cracking. The curves governed by bifurcation are simulated well by means of the so-called bifurcation equation, whereas such are not the case for those undergoing splitting or cracking due to premature failure. The need of the dual viewpoint of bifurcation and fracture in the compressive behavior of concrete has thus been clearly demonstrated.
Keywords: bifurcation, compressive failure

1 Introduction

The tensile failure of concretes has successfully been described by the fracture mechanics. Yet it is quite problematic to make clear the fundamental mechanism of their compressive failure that cannot be explained solely by the fracture mechanics.

(a) Bifurcation   (b) Splitting or cracking

Stress   Stress
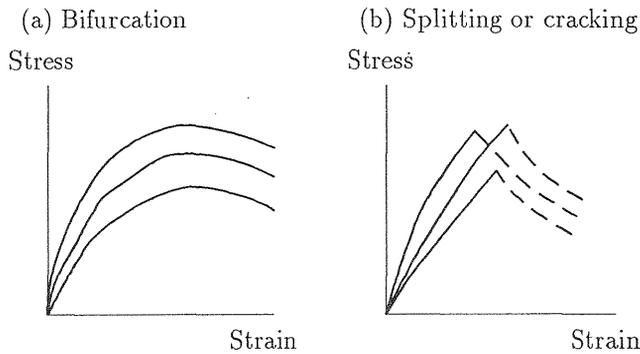
Figure 1 Classification of compressive failure mechanism.

A clue to overcome this problem can be found in the field of soil mechanics, in which "bifurcation" has come to be acknowledged as a major source of shear failure. For example, a shear band analysis of granular materials was performed by Vermeer (1982) as an extension of the plastic bifurcation by HIll and Hutchingson (1975). Ikeda and Goto (1993) and Ikeda et al. (1997a,b) employed imperfection sensitivity laws to assess the presence of bifurcation for sand specimens and to explain the variation of the shear strength of sand specimens. Furthermore, this method is successfully applied to the compressive failure of concretes by Ikeda and Maruyama (1995) and Ikeda et al. (1997c).

The aim of this paper is to make clear the fundamental mechanism of the compressive behavior of cylindrical concrete specimens reinforced by steel fibers through a dual viewpoint of bifurcation and fracture. The asymptotic bifurcation theory is employed as a means to testify if the bifurcation that triggers the softening of the stress versus strain curve is taking place for a specimen or not. By observing a series of compressive stress versus strain curves of those specimens based on this theory, we classified them into two categories: their peak loads are governed by (1) bifurcation and by (2) splitting or cracking, as shown in Fig. 1. Experimental data are shown to accurately follow the law for imperfection sensitivity. Further, we simulate the stress versus strain curves by means of the bifurcation equation. As a consequence of these, we assess the major assumption of the paper that the bifurcation is actually taking place in concrete specimens under compression.
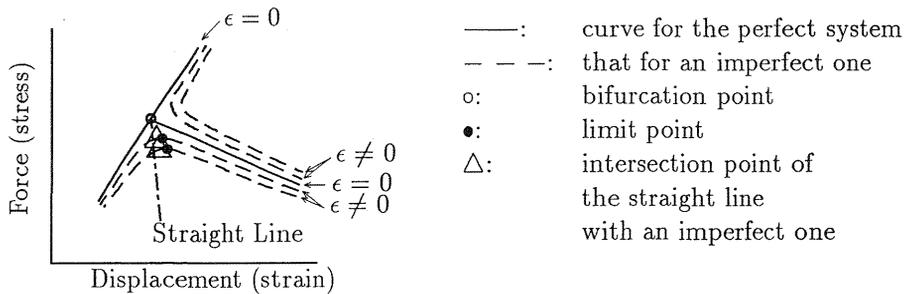
Figure 2   General view of force versus displacement curves for a bifurcation point.

2 Bifurcation Theory

In this section we offer a systematic means to describe the asymptotic influence of initial imperfections on the bifurcation behavior as a summary of Ikeda *et al.* (1997b). This serves as a synthesis and an extension of the pre-existing bifurcation theories, such as Koiter (1945), Thompson and Hunt (1973), and Ikeda *et al.* (1997a).

Consider a system of nonlinear equilibrium equations

$$\boldsymbol{F}(\boldsymbol{u}, P, \epsilon) = \boldsymbol{o}, \tag{1}$$

where $\boldsymbol{u}$ indicates a nodal displacement (or position) vector; P denotes a loading parameter (axial stress in this paper); ϵ denotes the magnitude of an initial imperfection. We assume $\boldsymbol{F}$ to be sufficiently smooth. We consider a bifurcation point $(\boldsymbol{u}_c^0, P_c^0)$ for the perfect system (shown as (o) in Fig. 2), at which the Jacobian $J^0 = (\partial \boldsymbol{F}/\partial \boldsymbol{u})^0$ becomes singular. Here $(\cdot)_c$ refers to the critical point and $(\cdot)^0$ to the perfect system.

2.1 Imperfection sensitivity laws
Imperfection sensitivity laws to testify the presence of bifurcation with reference to curves of experimental stress versus strain are introduced. The analyses presented in the sequel are all asymptotic and are valid only when ϵ is small.

We define the variables as below:

- $(\boldsymbol{u}_c^0, P_c^0)$: the bifurcation point (shown as (o) in Fig. 2),

- $(\boldsymbol{u}_c, P_c)$: the limit point for an imperfect one (shown as (•)),

- $\delta u = u_{i^*} - (u_{i^*})^0_c$: the increment of the displacement for a particular $i = i^*$ [$(u_{i^*})^0_c$ is abbreviated as u^0_c in the sequel],

- $\delta u_c = (u_{i^*})_c - (u_{i^*})^0_c$: the increment of the critical displacement,

- $\delta P = P - P^0_c$: the increment of the load, and

- $\delta P_c = P_c - P^0_c$: the increment of the critical load.

From the equilibrium equations (1), we can derive an incremental force versus displacement curve:

$$\sqrt{\text{sign}(s)\left(\delta u - \frac{\delta P}{E}\right)}\left[\delta P + p\left(\delta u - \frac{\delta P}{E}\right)\right] \pm q\epsilon + \text{h.o.t.} = 0, \quad (2)$$

where E is the parameter denoting the tangent of the main path of the perfect system; p is the parameter associated with the curvature of the bifurcation path; $q\epsilon$ represents the influence of the initial imperfection; $\text{sign}(s)$ is equal to 1 or -1; and h.o.t. means the higher order terms. It should be remarked that the applicability of equation (2) relies on the (reasonable) assumption that the bifurcation mode does not have the component of the displacement u.

In what follows, we consider an imperfect system with $\epsilon \neq 0$. First we remark that (2) readily implies

$$\delta P_c = -\text{sign}(s)\frac{3p^{1/3}q^{2/3}}{2^{2/3}}\epsilon^{2/3} + \text{h.o.t.}, \quad (3)$$

which is nothing but the famous Koiter's two-thirds power law (cf., Koiter, 1945).

We generalize the Koiter law (3) by considering a straight line

$$\delta P + h\delta u = 0 \quad (4)$$

shown by the dashed-and-dotted line in Fig. 2 (where h is a constant and $h = 3p/(1 - 3p/E)$ corresponds to the Koiter law). A substitution of the equation (4) of this straight line into (2) and the use of the Koiter law (3) results in

$$\delta P_c = -\gamma^*\delta u_{|h} + \text{h.o.t.} \quad (5)$$

where $\delta u_{|h}$ denotes the incremental displacement on the intersection point [shown as ($\triangle$) in Fig. 2] of the straight line (4) and an imperfect P versus u curve, and

$$\gamma^* = \frac{3}{2^{2/3}}\left[p\left(1 + \frac{h}{E}\right)\right]^{1/3}\left[-h + p\left(1 + \frac{h}{E}\right)\right]^{2/3}. \quad (6)$$

The equation (5) denotes a linear relationship between a pair of physically observable variables $\delta u_{|h}$ and δP_c that passes the origin $(\delta u_{|h}, \delta P_c) = (0,0)$. Namely, $(\delta u_{|h}, \delta P_c)$ for different values of ϵ all lie on the line (5) with a common slope $-\gamma^*$.

2.2 Determination of the values of parameters

In the application of the asymptotic formulas (2) and (5) to an experimental curve of a system subject to bifurcation, the values of the parameters p, $q\epsilon$, and E and the location (u_c^0, P_c^0) of the bifurcation point have to be estimated since it cannot be known *a priori*. A procedure to determine them is presented in this subsection.

A search type method is suggested for use in determining the locations of a few bifurcation points. The information to be extracted from the curve is the location $\delta u_{|h}$ of the intersection point of the straight line (4) and the curve for different values of the slope h of the line. This is based on the fact that the law (5) holds for any values of the slope h, say $(h_i \mid i = 1, 2, \cdots)$. If we employ a number of different values of h, we can estimate P_c^0, u_c^0, δP_c, p and E on the basis of the equation (5) from the observed values of $\delta u_{|h}$ for $h = h_1$, h_2, $\cdots$. To derive such estimates we could resort to least-square-type methods. In this paper we adopted the following somewhat *ad hoc* but an easy-to-implement method using four different values of h.

The use of the law (5) for two different values of $h = h_i$, h_j leads to

$$\frac{\delta u_{|h_i}}{\delta u_{|h_j}} = \frac{\gamma_j^*}{\gamma_i^*} = \frac{\left(1 + \dfrac{h_j}{E}\right)^{1/3}\left[-h_j + p\left(1 + \dfrac{h_j}{E}\right)\right]^{2/3}}{\left(1 + \dfrac{h_i}{E}\right)^{1/3}\left[-h_i + p\left(1 + \dfrac{h_i}{E}\right)\right]^{2/3}} \tag{7}$$

by equation (6). With the use of three different values of h, accordingly, the values of p and E are determined by equation (7). With four different values of h, we can arrive at four sets of three different values (h_2, h_3, h_4), (h_1, h_3, h_4), (h_1, h_2, h_4), and (h_1, h_2, h_3); accordingly, four different values of E, $(E_i \mid i = 1, \cdots, 4)$, are obtained. Then the location (u_c^0, P_c^0) can be determined as a point where the sample variance among $(E_i \mid i = 1, \cdots, 4)$ is minimized.

3 Compression Tests on Concrete Specimens

Compression test on cylindrical concrete specimens with a diameter of 10 cm and a height of 20 cm was conducted to obtain a series of
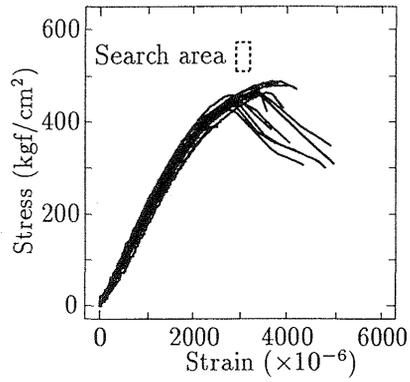
Figure 3   Stress versus strain $(\sigma - \varepsilon)$ curves for concrete specimens reinforced by steel fibers.

(a) Bifurcation

(b) Splitting or cracking
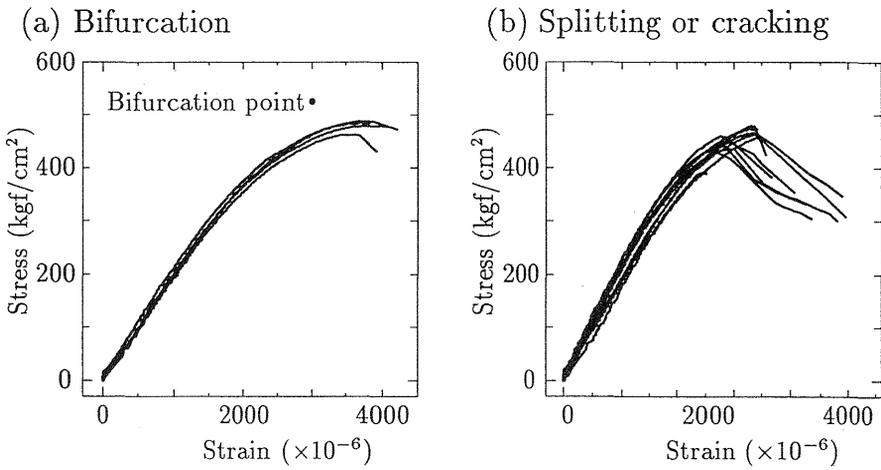
Figure 4   Classification of the stress versus strain $(\sigma - \varepsilon)$ curves in Fig. 3.

Bifurcation point(3016,525)

$-\log_{10}[Var[E]]$

2
1.5
1
0.5
0

Search area: $2900 < \epsilon < 3100 \ (\times 10^{-6})$, $510 < \sigma < 570 \ (\mathrm{kgf/cm^2})$
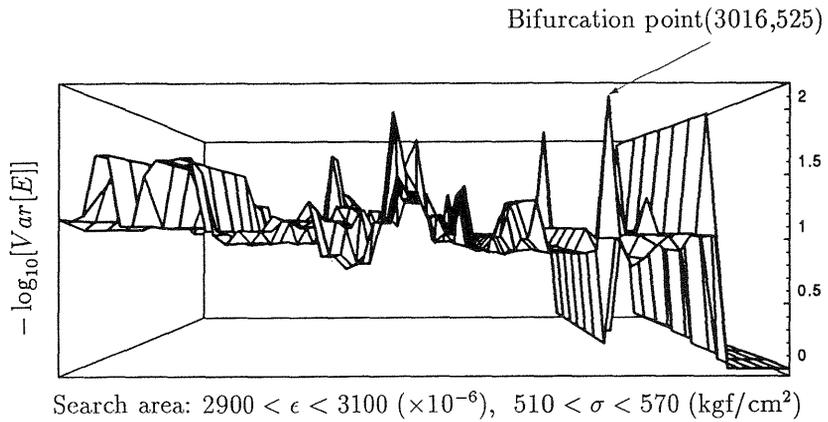
Figure 5 Contour map of sample variance $\mathrm{Var}E$ among E_i ($i = 1, \cdots, 4$).

compressive stress versus axial strain $(\sigma - \varepsilon)$ curves in Fig. 3. The mix proportion is listed in Table 1. In order to avoid premature splitting or cracking, these specimens were reinforced by the use of 0.5 % steel fibers, which are of the length of 29 mm and of the diameter of 0.5 mm with hooks at both ends. These curves are investigated in the sequel by means of the method introduced in the previous section, which holds also for this case merely by replacing

$$P \to \sigma, \quad u_i \to \varepsilon. \tag{8}$$

Table 1 The mix proportion for the experimental specimens.

w/c (%)	s/a (%)	Unit content $(\mathrm{kg/m^3})^*$			AE ($\% -c$)
		w	c	s	
50	100	313	625	1255	0.01

* $\mathrm{1lb/ft^3} = 16.02\mathrm{kg/m^3}$.

The stress versus strain $(\sigma - \varepsilon)$ curves in Fig. 3 were classified[1] into two types as shown in Fig. 4, according to whether their peak loads are governed by (a) bifurcation or by (b) splitting or cracking (cf., Fig. 1).

The technique of the search of the bifurcation point presented in §2.2 is applied to a stress versus strain curve in Fig. 4(a), whose

---

[1]The development of a more systematic means for the classification is the topic requiring further studies.
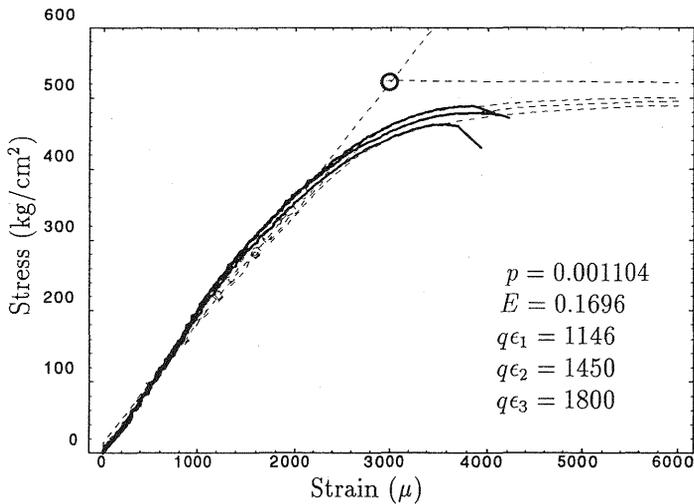
Figure 6　Simulation of stress versus strain curves. o: bifurcation point.

peak is governed by the bifurcation. The rectangular area in Fig. 3 denotes the search area employed, whereas Fig. 5 shows the contour map of the sample variance among E_i $(i = 1, \cdots, 4)$ in the rectangular area. Figure 5 clearly shows the presence of the local minimum, where the bifurcation point is located. At the course of this search to locate the bifurcation point, the values of the parameters shown in Fig. 6 were determined. Figure 6 shows the simulation of the experimental stress versus strain $(\sigma\text{-}\varepsilon)$ curves of three representative sets of specimens. It is to be noted that, in agreement with the concept of the present theory, the same set of the values of the parameters but different values of the initial imperfection ϵ were employed for these specimens. The theoretical curves correlate fairly well with the experimental ones.

We plot in Figure 7 the incremental strain $(\delta\varepsilon_a)_{|h}$ versus incremental maximum stress $|\delta\sigma_c| = |\sigma_c - \sigma_c^0|$ interrelationships, where R is the reliability coefficient and (a) corresponds to all curves in Fig. 3 and (b) to those in Fig. 4(a) subject to bifurcation. The relationship in (b) accurately follows the imperfection sensitivity law (5), which corresponds to the straight lines in this figure. Moreover, the

342

(a) All ($h = 0.1$) (b) Bifurcation
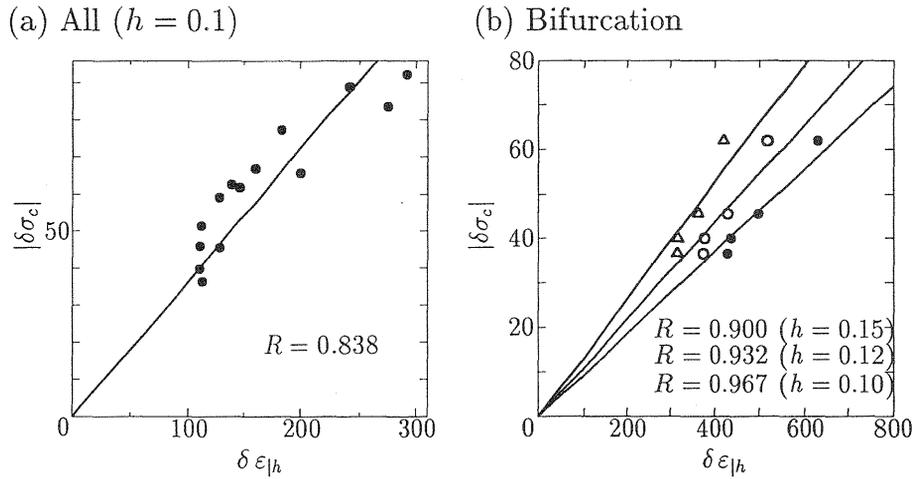
Figure 7 $|\delta P_c|$ versus $\delta\varepsilon_{|h}$ relationships.

value of reliability coefficient for (b) is greater that that for (a), in agreement with the fact that the law (5) holds for systems subject to bifurcation. This testifies the validity of the present method, which explains the variation of the curves of concretes by the variation of initial imperfections.

5 Conclusion
As we have seen, the bifurcation and splitting or cracking is the two major causes of the failure of concrete specimens. The reinforcing of concrete specimens by steel fibers has prevented premature cracking and made clear the presence of bifurcation that hitherto has been disregarded. A future study on the compressive strengt of concretes should be made based on the viewpoint of bifurcation so as to arrive at the true constitutive relationships.

6 Acknowledgements

7 References

Hill, R. and Hutchinson, J.W. (1975) Bifurcation phenomena in the plane tension test. **J. Mech. & Phys. Solids**, 23, 239–264.

Ikeda, K., Chida, T. and Yanagisawa, E. (1997a) Imperfection sensitive strength variation of soil specimens. **J. Mech. & Phys. Solids**, 45(2), 293–315.

Ikeda, K. and Goto, S. (1993) Imperfection sensitivity for size effect of granular materials. **Soils & Foundations,** 33(2), 157–170.

Ikeda, K., Murota, K., Yamakawa, Y. and Yanagisawa, E. (1997b) Mode switching and recursive bifurcation in granular materials. **J. Mech. & Phys. Solids**, 45/11-12, 1929–1953.

Ikeda, K. and Maruyama, K. (1995) Compressive strength variation of concrete specimens due to imperfection sensitivity. **Fracture Mech. Concrete Structures, Proc. FRAMCOS-2**, F.W. Wittmann ed., Vol. 1, 425–434.

Ikeda, K., Maruyama, K., Ishida, H. and Kagawa, S. (1997c) Bifurcation in compressive behavior of concrete. **ACI Materials J.,** 94(6) 484–491.

Koiter, W.T. (1945) On the stability of elastic equilibrium, **Dissertation. Delft, Holland,** (English translation: NASA Tech. Trans. F10: 833, 1967).

Thompson, J.M.T. and Hunt, G.W. (1973) **A General Theory of Elastic Stability.** John Wiley and Sons, New York.

Vermeer, P.A. (1982) A simple shear-band analysis using compliances. **IUTAM, Conf. Deformation & Failure Granular Materials,** 493–499.